arXiv:1607.07587v1 [cond-mat.soft] 26 Jul 2016

Nonequilibrium self-organization of colloidal particles on substrates: adsorption, relaxation, and annealing

Nuno A. M. Araújo, Cristóvão S. Dias, Margarida M. Telo da Gama

Centro de Física Teórica e Computacional, Faculdade de Ciências, Universidade de Lisboa, Portugal

Departamento de Física, Faculdade de Ciências, Universidade de Lisboa, Portugal

E-mail: nmaraujo@fc.ul.pt

July 2016

Abstract. Colloidal particles are considered ideal building blocks to produce materials with enhanced physical properties. The state-of-the-art techniques for synthesizing these particles provide control over shape, size, and directionality of the interactions. In spite of these advances, there is still a huge gap between the synthesis of individual components and the management of their spontaneous organization towards the desired structures. The main challenge is the control over the dynamics of self-organization. In their kinetic route towards thermodynamically stable structures, colloidal particles self-organize into intermediate (mesoscopic) structures that are much larger than the individual particles and become the relevant units for the dynamics. To follow the dynamics and identify kinetically trapped structures, one needs to develop new theoretical and numerical tools. Here we discuss the self-organization of functionalized colloids (also known as patchy colloids) on attractive substrates. We review our recent results on the adsorption and relaxation and explore the use of annealing cycles to overcome kinetic barriers and drive the relaxation towards the targeted structures.

1. Introduction

Colloidal particles have a typical size ranging from the micron down to the nanometer scale. With state-of-the-art techniques, it is possible to synthesize them monodisperse in shape and size [1, 2], spherical or asymmetric in shape [3], and to fine tune their pairwise interactions [4, 5]. These impressive experimental advances have turned colloidal particles into ideal building blocks to produce a new generation of materials with enhanced physical properties [6, 7, 8]. At the colloidal scale, mechanical and optical properties are strongly sensitive to the particles spatial arrangement. So, there are two main challenges: the identification of target structures yielding the desired properties and the design of pathways to synthesize them. By gripping and releasing

colloidal particles with the tip of a microscope some target structures can be obtained [9], but this is an expensive strategy limited to very simple configurations and rather small structures [10]. Thus, the ultimate goal of Soft Matter is to produce the desired structures through self-assembly without individual control of the particles positions [11, 12].

The controlled self-organization of colloidal particles into large-scale structures is still an experimental and theoretical challenge. Most theoretical studies have considered equilibrium conditions. Experimentally, this assumption would imply that the characteristic time of the external perturbations is much larger than the necessary time to relax towards equilibrium. Such studies benefit from a well-established theoretical framework and provide valuable information on the system free energy, self-healing mechanisms, and aging. However, in practice, equilibrium is an exception rather than the rule. Real structures are typically obtained under nonequilibrium conditions and the kinetics of growth and relaxation cannot be neglected. In particular, colloidal particles usually self-organize into mesoscopic kinetic structures much larger than the individual constituents. Their relaxation involves concerted moves and thus, the lifetime of each state increases strongly with the number of constituents. When such structures span the entire system, for example, a gel, the lifetime may diverge with the system size and the access to the thermodynamic structures is strongly compromised [13, 14, 15]. The probability of observing a given kinetic structure is not necessarily dependent on its absolute free energy, but mainly on the size and accessibility of its basin of attraction in the energy manifold. For very corrugated energy landscapes, the system explores the energy manifold through thermally activated processes, hoping from basin to basin, where the mean residence time in each state depends on the possible paths to leave it and their corresponding energy barriers. New numerical and theoretical tools are then needed to investigate how competing timescales take the system away from equilibrium and to provide insight on the feasibility of the thermodynamic structures.

As an example, we consider the self-organization of colloidal particles on attractive substrates when relaxation is slower than aggregation, so the emerging kinetically trapped (percolating) structures prevent the evolution towards equilibrium. Studies of self-assembly have focused on the bulk, neglecting boundary effects. Yet, the presence of a surface improves the control over aggregation [16, 17, 18, 19, 20, 21, 22, 23]. For example, in the limit of irreversible binding, the assembled structures differ dramatically from the thermodynamic ones [24, 25, 26, 27]. We also consider colloidal particles with limited valence, known as patchy colloids. The absence of directional links in isotropic colloids limits the control of the final structure [28, 5]. By contrast, patchy colloids, decorated with n attractive patches on their surface, permit a fine control of colloidal valence and of the local arrangements. They are a powerful tool for engineering the assembly of target structures and give the possibility of obtaining very-low-density networks of connected particles, which form gels [29, 30]. In the last years, experimental and theoretical studies have investigated how the number, type, and distribution of patches can affect the aggregation process and, consequently, the

assembled structures [31, 32, 33, 34, 35, 36]. It has been reported that controlling the valence, allows tuning the density and temperature of both the gas-liquid and sol-gel transitions [37, 35]. Patchy models with n lower than 12 have been shown to disfavor dense local configurations, broadening the region of stability of the liquid phase in the temperature-density plane [38].

The manuscript is organized in the following away. We discuss the limit of irreversible adsorption in Sec. 2 and the dynamics of relaxation in Sec. 3. The possibility of using annealing cycles to relax kinetically trapped structures is discussed in Sec. 4. We make some final remarks in Sec. 5.

2. Irreversible adsorption

The dynamics of colloidal particles on substrates results from a balance between the adsorption/desorption of particles and the aggregation/relaxation of the colloidal structures. Let us consider strongly attractive substrates, such that desorption is practically negligible within the timescale of interest. Thus, the number of colloidal particles on the substrate increases monotonically in time. The relevant timescale is the inter-arrival time (inverse flux), which corresponds to the typical time between two adsorption events and should depend on the concentration and mobility of the colloidal particles in solution (bulk). The aggregation/relaxation is a more complex process. Initially, it depends only on the number and diffusion coefficient of the particles on the substrate. As the dynamics evolves, aggregates of different size and shape are formed leading to a hierarchy of relaxation times. While diffusion of individual particles occurs in the Brownian timescale (of the order of a second), the relaxation of aggregates might take hours or even days.

To study the role of limited valence and the directionality of interactions on the adsorption of patchy particles on substrates, we have considered, as a first approximation, the limit of irreversible adsorption [39, 40, 41, 42, 43, 44, 45, 46]. The inter-arrival time is much shorter than any relaxation timescale and thus the particles are considered immobile once adsorbed on the substrate. To address this limit, we have proposed a discrete kinetic model for aggregation that is a generalization of the well-known ballistic deposition model to include the directionality of interactions [47]. Accordingly, particles are considered spherical with n patches equally spaced on their surface. The particle-particle interaction is pairwise and it is described as an excluded volume interaction. The patch-patch interaction is short range and described in a stochastic way, as explained next. We assume that patches of two different colloids can form bonds only upon collision. We define an interaction range on the surface of the colloidal particle, surrounding each patch, parameterized by an angle θ. When two particles collide, if the contact point is within the interaction range of their patches, then the two particles form an irreversible bond mediated by these patches. In the simulation, since only one colloid moves at a time, the formation of a bond occurs stochastically with probability p, when the moving particle collides within the interaction range of a

patch of the immobile one. p corresponds to the fraction of the surface of the moving particle covered by the interaction range of all n patches.

Particles are sequentially released from a random position above the growth front and move ballistically (vertically) towards the substrate. If they hit the substrate without overlapping any previously adsorbed particle, they immediately stick to it irreversibly with a random orientation. However, if they collide first with a previously adsorbed particle, the pairwise interaction described previously is considered. If the formation of a bond is not successful, the particle is discarded and a new one is released from a random position above the growth front.

By neglecting any relaxation, it is possible to access very large length and timescales. Performing kinetic Monte Carlo simulation, we were able to show that the kinetic structures are significantly different from the thermodynamic ones and that they depend strongly on the number of patches [26, 48], patch-patch correlations [49, 27, 50], and mechanism of mass transport [47]. We have also identified a very rich critical behavior of the interfacial properties. In the simplest case of three-patch particles, we have found two new absorbing phase transitions depending on the opening angle between the patches [49]. A careful scaling analysis reveals that one of these absorbing phase transitions changes from discontinuous to continuous at a tricritical flexibility of the bonds [51]. We have also extended our stochastic model to study particles with distinct patch-patch interactions [27, 50]. For particles with two types of patches, we reported a crossover of the interfacial roughness from the Kardar-Parisi-Zhang (KPZ) to the KPZ with quenched disorder (KPZQ) universality class when the difference between the strong and weak bonds is sufficiently large [50, 51].

3. Relaxation dynamics

For sufficiently weak particle-particle interactions or long timescales, the non-equilibrium structures discussed in the previous section are expected to relax and eventually reach equilibrium. To study such relaxation dynamics, we consider now a three-dimensional system of spherical colloidal particles, with three patches equally distributed along the equator. To follow the individual particles, we performed Langevin dynamics simulations using LAMMPS [52]. As we proposed in Ref. [13], colloidal particles are described as spheres of radius R and mass m_c with three patches fixed at a distance R from the center, forming an opening angle of $2\pi/3$. The particles representing the patches are of zero diameter and mass $10^{-5}m_c$, which is practically negligible for the dynamics. Their relative position to the center of the core is fixed at all times. The interaction between colloids is repulsive, described by a Yukawa potential,

$$V_{\text{rep}} = \frac{A}{k} \exp\left\{-k\left[r - (R_i + R_j)\right]\right\}, \tag{1}$$

where r is the distance between the center of the particles, R_i and R_j are the effective radii of the two interacting particles, $A = 1$ is the interaction strength (in units of $k_BT/2R$) and $k = 40$ the inverse of the screening length (in units of the inverse particle

diameter $(2R)^{-1}$); the interaction between patches is described by an attractive inverted Gaussian potential [13, 53], defined as,

$$V_{\rm att} = -\epsilon \exp\left(-\sigma r_p^2\right), \tag{2}$$

where $\epsilon = 40$ (in units of k_BT) is the interaction strength and $\sigma = 10^2$ in units of the inverse squared particle diameter.

The isotropic particle-substrate interaction is obtained from the Hamaker theory for two spheres [54] in the limit where the radius of one of the particles diverges. This gives an attractive $V_{\rm s,att}$ and a repulsive $V_{\rm s,rep}$ potential, defined as,

$$V_{\rm s,att} = -\frac{A_H}{6}\left[\frac{2R}{D}\frac{R+D}{D+2R} + \ln\left(\frac{D}{D+2R}\right)\right], \tag{3}$$

and

$$V_{\rm s,rep} = \frac{A_H\sigma^6}{7560}\left(\frac{6R-D}{D^7} + \frac{D+8R}{(D+2R)^7}\right), \tag{4}$$

respectively, where A_H is the Hamaker's constant and D the distance between the surface of the particle and the substrate.

To resolve the stochastic trajectories of the particles, we integrated the corresponding Langevin equations of motion for the translational and rotational degrees of freedom,

$$\begin{aligned} m\dot{\vec{v}}(t) &= -\nabla_{\vec{r}}V(\vec{r},\vec{\theta}) - \frac{m}{\tau_t}\vec{v}(t) + \sqrt{\frac{2mk_BT}{\tau_t}}\vec{\xi}(t), \\ I\dot{\vec{\omega}}(t) &= -\nabla_{\vec{\theta}}V(\vec{r},\vec{\theta}) - \frac{I}{\tau_r}\vec{\omega}(t) + \sqrt{\frac{2Ik_BT}{\tau_r}}\vec{\xi}(t), \end{aligned} \tag{5}$$

where, $\vec{v}$ and $\vec{\omega}$ are the translational and angular velocities, m and I are the mass and inertia of the colloidal particles, V is the pairwise potential, and $\vec{\xi}(t)$ is the stochastic term drawn from a random distribution with zero mean. We considered a relation between damping times $\tau_r = 10\tau_t/3$. For the sake of generality, time is given in units of the Brownian time, defined as $\tau_B = (2R)^2/D_t$, where $D_t = k_BT\tau_t/m_c$ is the translational diffusion coefficient.

The initial structures were obtained with the stochastic model described in the previous section. They consist of 5120 particles adsorbed on a substrate of lateral size $L = 16$, in units of the particle diameter. For the dynamics, we considered $\tau_t = 0.1$ and $k_BT = 1$. Figure 1 shows, for different instants of time, (a) the particle density $\rho^*(z)$, defined as the number of particles per unit volume, and (b) the bond density $\rho_c(z)$, as a function of the distance to the substrate z. While the particle density profile does not change significantly in time, the bond density does increase by more than 40%. Fig. 2 depicts snapshots at the same instants, where the number of bonds per particle is indicated by the particle color. For the thermostat temperature considered, no bond breaking is observed within the time scale of the simulation ($10^3\tau_B$). Rather, the relaxation dynamics is driven by the formation of new bonds, maximizing the number of bonds per particle. As one starts from a singly connected, tree-like structure, loops are

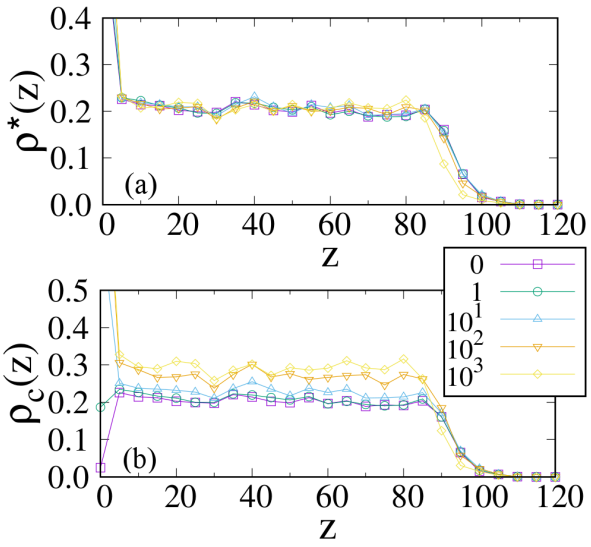

Figure 1. (a) Particle and (b) bond density as a function of the distance to the substrate z, at different times, for an initial structure consisting of 5120 patchy particles adsorbed on an attractive substrate, obtained with the stochastic model described in Sec. 2. Results are averages over 10 samples, for patchy particles adsorbed on a substrate of lateral size $L = 16$, in units of the particle diameter.

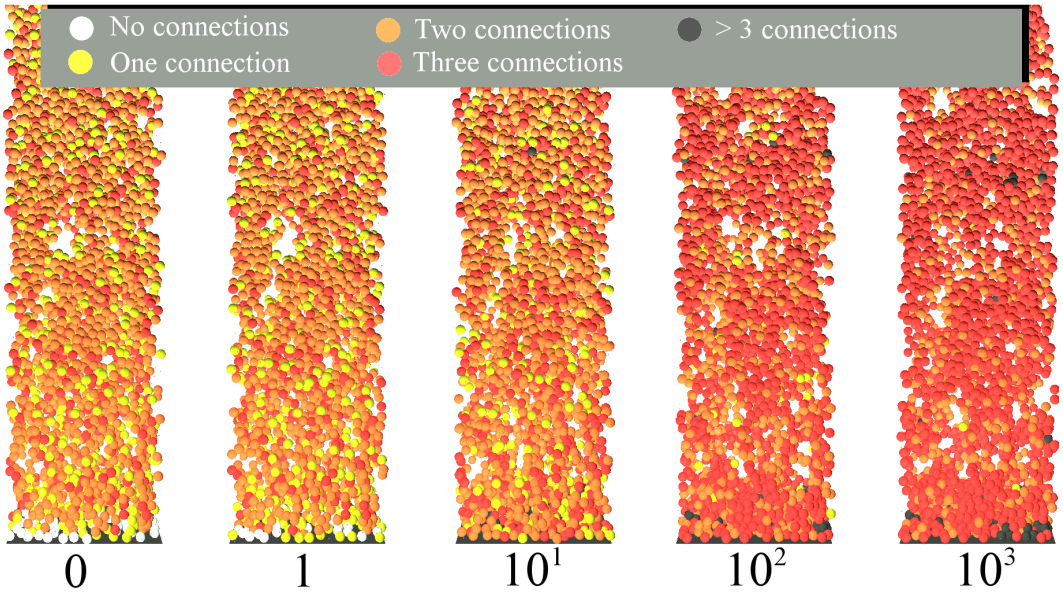

Figure 2. Snapshots for 5120 patchy particles on a substrate of lateral size $L = 16$, in units of the particle diameter. Snapshots are at different instants of time, namely, $t = \{0, 1, 10, 10^2, 10^3\}$, in units of the Brownian time τ_B. The color of each particle indicates its number of bonds.

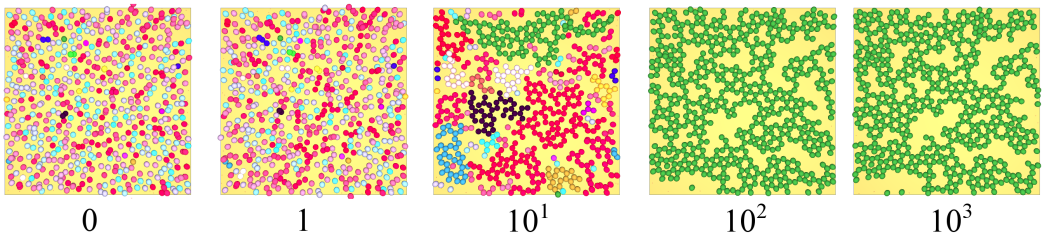

Figure 3. Snapshots for 614 patchy particles adsorbed on a substrate of lateral size $L = 32$, in units of the particle diameter, at different instants of time, namely, $t = \{0, 1, 10, 10^2, 10^3\}$, in units of the Brownian time τ_B. Different colors are different aggregates of connected particles.

formed every time a new bond is established, which is expected to affect the mechanical properties of the colloidal network.

To characterize the initial stage of adsorption, in Ref. [13], we focused on the submonolayer regime, where the number of adsorbed particles is not enough to completely cover the substrate. We found that, even in this case, the relaxation towards thermodynamic phases is hindered by the formation of kinetically trapped structures that are stable over long timescales (see Fig. 3). From the time evolution of the number of different aggregates N_s, we identified two relaxation regimes. Initially, N_s decays exponentially with time (see Fig. 4(a)), with a characteristic time that decays linearly with the number of adsorbed particles in the submonolayer regime. This fast relaxation is essentially driven by the diffusion and aggregation of initially isolated particles [13]. As the number of such isolated particles vanishes, the evolution of $N_s(t)$ towards its asymptotic value $N_s(\infty) = 1$ is much slower, as shown in Fig. 4(b). For values of the coverage below the percolation threshold, the numerical data is consistent with a scale-free relaxation, with an exponent 0.8 ± 0.1, independent of the value of the coverage. Above the percolation threshold, a single cluster is rapidly formed, with a structure that is significantly different from the thermodynamic one.

4. Annealing cycles

Adsorbed particles diffuse and form patch-patch bonds with other particles. For the mechanical stability of the final structures, it is key that these bonds are strong enough; but strong bonding compromises significantly the relaxation dynamics. For example, DNA mediated bonds are practically irreversible within the time scale of interest [55, 43, 46, 23, 30]. In this limit, kinetically arrested structures are formed that differ significantly from the thermodynamic ones [13, 30].

One promising strategy to overcome these arrested structures is to design protocols of switching on/off the patch-patch bonds [41, 56, 40, 55, 42]. For example, DNA mediated bonds are characterized by a sharp transition in the bonding probability at their dissociation (or melting) temperature. Thus, bonds can be effectively switched

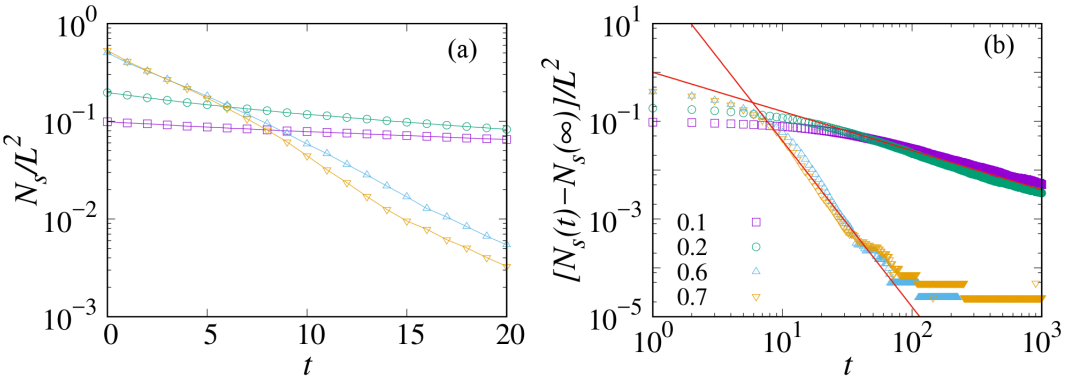

Figure 4. (a) Time evolution of the number of aggregates N_s for different initial coverages $\theta = N\pi/4$, defined as the ratio of the total area of the cross-section of all adsorbed particles and the area of the substrate, with $N = \{0.1, 0.2, 0.6, 0.7\}$. (b) Approach to the asymptotic value $N_s(\infty) = 1$. Results are averages over 10 samples on substrates of lateral size $L = 64$, in units of the particle diameter.

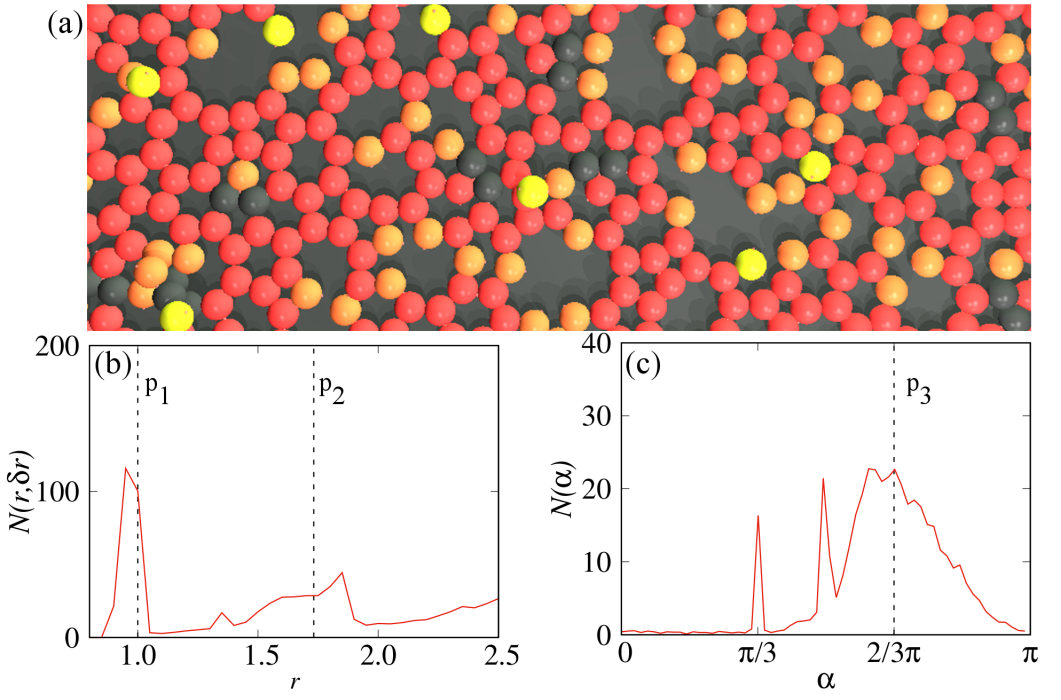

Figure 5. (a) Snapshot, (b) radial and (c) angular distribution functions for a coverage of $\pi/[3\tan(\pi/3)]$, corresponding to a honeycomb lattice. The vertical dashed lines correspond to the expected peaks (p_1, p_2, p_3) for a honeycomb lattice: $r = 1$, $r = \sqrt{3}$, and $\alpha = 2\pi/3$. Results are averages over 20 samples on substrates of lateral size $L = 32$, in units of the particle diameter, after $t = 10^3$, in units of the Brownian time τ_B, with $\delta r = 0.1$ in Eq. (6).

on/off by performing temperature annealing cycles around the melting temperature.

To explore this possibility, we consider now the same system, but start from a number of adsorbed patchy particles that correspond to the coverage of the honeycomb

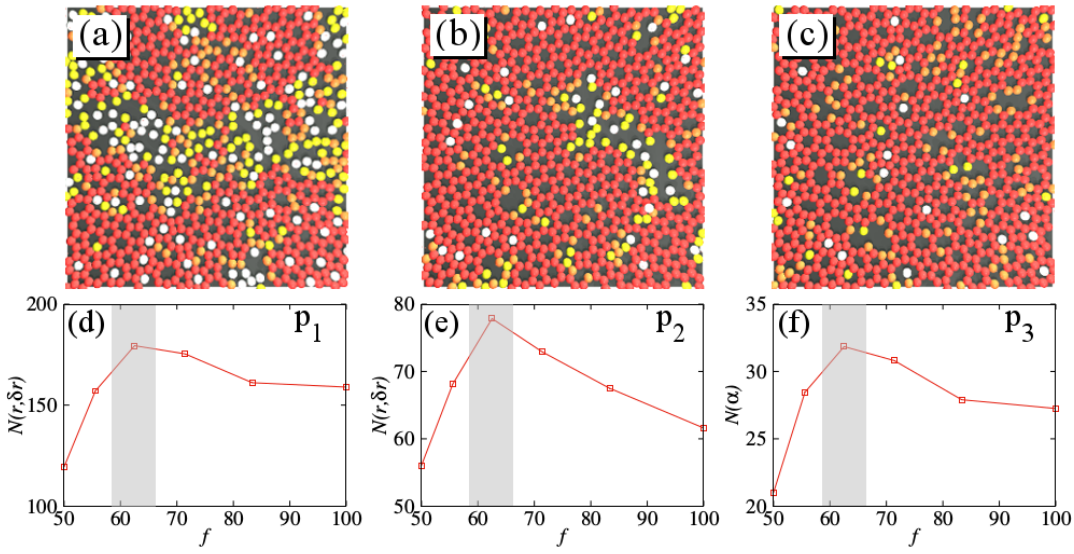

Figure 6. Snapshots for different annealing frequencies f, namely, (a) 50, (b) 62.5, and (c) 100, in units of τ_B^{-1}. Value of the radial/angular distribution functions at the peaks (d) p_1, (e) p_2, and (f) p_3, in Fig. 5, as a function of the annealing frequency f. Results are averages over 20 samples on substrates of lateral size $L = 32$, in units of the particle diameter, for $t = 3000\tau_B$. The system is initially relaxed for $1000\tau_B$, and the annealing cycles are performed for more $2000\tau_B$ time units.

lattice, $\pi/\left[3\tan\left(\pi/3\right)\right]$. Figure 5(a) shows a snapshot obtained after relaxing for $10^3\tau_B$. Figure 5(b) is the radial distribution functions, defined as,

$$N(r,\delta r) = \sum_{i}^{N_p-1}\sum_{j>i}^{N_p} g\left(r_{ij}-r,\delta r\right)/r, \tag{6}$$

where, N_p is the total number of particles, r_{ij} is the distance between each pair ij of particles and $g\left(r_{ij}-r,\delta r\right)$ is one, if $|r_{ij}-r|<\delta r$, and zero, otherwise. For a honeycomb lattice we expect two peaks: at $r=1$ and $r=\sqrt{3}$, corresponding to the dashed lines p_1 and p_2, respectively. Instead, we observe a much broader distribution. Figure 5(c) is an angular distribution function for the patch-patch bond orientation, where α is the angle between two bonds of the same particle. A honeycomb lattice is characterized by a peak (p_3) at $\alpha = 2/3\pi$. Clearly, due to thermal fluctuations and practically irreversible bonds, the obtained structure differs significantly from the honeycomb lattice.

To illustrate the advantage of annealing cycles, after an initial relaxation for $10^3\tau_B$ we performed annealing cycles for an additional period of $2000\tau_B$. Accordingly, the patch-patch interaction is switched off for periods of $(2f)^{-1}$, followed by a period of the same length where the patch-patch interaction is on. Thus, f is the frequency of the annealing cycle in units of τ_B^{-1}. Figures 6(d)-(e) show the dependence of the peaks of the radial and angular distribution functions on f. We find an optimal value of $f\approx 60$, where the intensity of the peaks is maximized.

We hypothesize that the optimal frequency results from two competing mechanisms:

The rotational and the translational diffusions. While the former dominates at higher frequencies; the latter is the dominant one at lower ones. At high frequencies, the time interval for which the interaction is off is not long enough for the orientation of two previously connected patches to decorrelate or two new patches to align. This alignment is indeed a key mechanism for a particle with only two bonds to form a third one, since the spatial constraints imposed by the two connections significantly hinder relaxation. At low frequencies, the particle-particle correlations decay drastically before bonds are switched on again and, at every bond-on period of the cycle the dynamics resembles that at the initial relaxation time.

5. Final remarks

The dynamics of adsorption and relaxation of patchy particles on substrates is very rich, involving a hierarchy of processes occurring at different (length and time) scales. With a stochastic model of aggregation, it is possible to access the very long scales necessary to observe critical interfacial phenomena. Studies of the stochastic (Langevin) dynamics revealed a fast and slow relaxation. The latter stems from the formation of mesoscopic kinetic structures, the very slow relaxation of which involves concerted moves, and thus compromises the feasibility of the thermodynamic structures.

To overcome these kinetically arrested structures and relax the system towards the target structures, we have explored the use of annealing cycles of switching patch-patch interactions on and off. Numerical results suggest an intermediate optimal frequency at which the target structural properties are maximized in a given time. Future work should further explore further this possibility. It is important to characterize how this optimal frequency depends on the number of patches, parameters of the particle-particle, patch-patch, and particle-substrate interaction potentials, and on the number of adsorbed particles.

Studies of colloidal particle adsorption on substrates are of scientific and technological interest. From the theoretical perspective, they are prototypical examples of collective dynamics under confinement and require concepts such as competing time and length scales, many-body correlation, percolation and aging. For practitioners, they provide valuable information on this feasibility of thermodynamic structures and on how to design protocols to effectively drive colloidal self-organization towards the target structures.

Acknowledgments

We acknowledge financial support from the Portuguese Foundation for Science and Technology (FCT) under Contracts nos. EXCL/FIS-NAN/0083/2012, UID/FIS/00618/2013, and IF/00255/2013.

References

[1] Matijevic E 2011 *Fine particles in medicine and pharmacy* (New York: Springer)
[2] Halámek J, Zhou J, Halámková L, Bocharova V, Privman V, Wang J and Katz E 2011 *Anal. Chem.* **83** 8383
[3] Sacanna S and Pine D J 2011 *Curr. Op. Coll. Interf. Sci.* **16** 96
[4] Yethiraj A and van Blaaderen A 2003 *Nature* **421** 513
[5] Duguet E, Désert A, Perro A and Ravaine S 2011 *Chem. Soc. Rev.* **40** 941
[6] Doppelbauer G, Bianchi E and Kahl G 2010 *J. Phys.: Cond. Matt.* **22** 104105
[7] Glotzer S C and Solomon M J 2007 *Nat. Mater.* **6** 557
[8] Frenkel D and Wales D J 2011 *Nat. Mater.* **10** 410
[9] Kufer S K, Puchner E M, Gumpp H, Liedl T and Gaub H E 2008 *Science* **319** 594
[10] Parak W J 2011 *Science* **334** 1359
[11] Whitesides G M and Grzybowski B 2002 *Science* **295** 2418
[12] Ma H and Hao J 2011 *Chem. Soc. Rev.* **40** 5457
[13] Dias C S, Braga C, Araújo N A M and Telo da Gama M M 2016 *Soft Matt.* **12** 1550
[14] Chakrabarti D, Kusumaatmaja H, Rühle V and Wales D J 2014 *Phys. Chem. Chem. Phys.* **16** 5014
[15] Zaccarelli E, Saika-Voivod I, Buldyrev S V, Moreno A J, Tartaglia P and Sciortino F 2006 *J. Chem. Phys.* **124** 124908
[16] van Blaaderen A, Ruel R and Wiltzius P 1997 *Nature* **385** 321
[17] Cadilhe A, Araújo N A M and Privman V 2007 *J. Phys.: Cond. Matter* **19** 065124
[18] Kinge S, Crego-Calama M and Reinhoudt D N 2008 *ChemPhysChem* **9** 20
[19] Einstein T L and Stasevich T J 2010 *Science* **327** 423
[20] Ganapathy R, Buckley M R, Gerbode S J and Cohen I 2010 *Science* **327** 445
[21] Bernardino N R and Telo da Gama M M 2012 *Phys. Rev. Lett.* **109** 116103
[22] Gnan N, de las Heras D, Tavares J M, Telo M M and Sciortino F 2012 *J. Chem. Phys.* **084704** 084704
[23] Joshi D, Bargteil D, Caciagli A, Burelbach J, Xing Z, Nunes A S, Pinto D E P, Araújo N A M, Bruijc J and Eiser E 2016 *Sci. Adv.* **2** e1600881
[24] Araújo N A M, Cadilhe A and Privman V 2008 *Phys. Rev. E* **77** 031603
[25] Marques J F, Lima A B, Araújo N A M and Cadilhe A 2012 *Phys. Rev. E* **85** 61122
[26] Dias C S, Araújo N A M and Telo da Gama M M 2013 *Phys. Rev. E* **87** 032308
[27] Dias C S, Araújo N A M and Telo da Gama M M 2013 *Soft Matt.* **9** 5616
[28] Pawar A B and Kretzschmar I 2010 *Macromol. Rapid Commun.* **31** 150
[29] Zaccarelli E 2007 *J. Phys.: Condens. Matter* **19** 323101
[30] Dias C S, Tavares J M, Araujo N A M and Telo da Gama M M arxiv: 1604.05279
[31] Kretzschmar I and Song J H 2011 *Curr. Op. Coll. Interf. Sci.* **16** 84
[32] Sciortino F, Bianchi E, Douglas J F and Tartaglia P 2007 *J. Chem. Phys.* **126** 194903
[33] Bianchi E, Tartaglia P, La Nave E and Sciortino F 2007 *J. Phys. Chem. B* **111** 11765
[34] Bianchi E, Tartaglia P, Zaccarelli E and Sciortino F 2008 *J. Chem. Phys.* **128** 144504
[35] Russo J, Tartaglia P and Sciortino F 2009 *J. Chem. Phys.* **131** 014504
[36] Ruzicka B, Zaccarelli E, Zulian L, Angelini R, Sztucki M, Moussaïd A, Narayanan T and Sciortino F 2011 *Nature Mater.* **10** 56
[37] Bianchi E, Largo J, Tartaglia P, Zaccarelli E and Sciortino F 2006 *Phy. Rev. Lett.* **97** 168301
[38] Bianchi E, Blaak R and Likos C N 2011 *Phys. Chem. Chem. Phys.* **13** 6397
[39] Lee G U, Chrisey L A and Colton R J 1994 *Science* **266** 771
[40] Mirkin C A, Letsinger R L, Mucic R C and Storhoff J J 1996 *Nature* **382** 607
[41] Nykypanchuk D, Maye M M, van der Lelie D and Gang O 2008 *Nature* **451** 549
[42] Di Michele L, Fiocco D, Varrato F, Sastry S, Eiser E and Foffi G 2014 *Soft Matt.* **10** 3633
[43] Wang Y, Breed D R, Manoharan V N, Feng L, Hollingsworth A D, Weck M and Pine D J 2012

Nature **491** 51
[44] Biancaniello P L, Kim A J and Crocker J C 2005 *Phys. Rev. Lett.* **94** 058302
[45] Roldán-Vargas S, Smallenburg F, Kob W and Sciortino F 2013 *Sci. Rep.* **3** 2451
[46] Leunissen M E and Frenkel D 2011 *J. Chem. Phys.* **134** 084702
[47] Dias C S, Araújo N A M and Telo da Gama M M 2013 *J. Chem. Phys.* **139** 154903
[48] Dias C S, Araújo N A M and Telo da Gama M M 2015 *Mol. Phys.* **113** 1069
[49] Dias C S, Araújo N A M and Telo da Gama M M 2014 *Phys. Rev. E* **90** 032302
[50] Dias C S, Araújo N A M and Telo da Gama M M 2014 *Europhys. Lett* **107** 56002
[51] Araújo N A M, Dias C S and Telo da Gama M M 2015 *J. Phys.: Cond. Matt.* **27** 194123
[52] Plimpton S 1995 *J. Comp. Phys.* **117** 1
[53] Vasilyev O A, Klumov B A and Tkachenko A V 2013 *Phys. Rev. E* **88** 012302
[54] Everaers R and Ejtehadi M R 2003 *Phys. Rev. E* **67** 041710
[55] Geerts N and Eiser E 2010 *Soft Matt.* **6** 4647
[56] Malinge J, Mousseau F, Zanchi D, Brun G, Tribet C and Marie E 2016 *J. Colloid Interf. Sci.* **461** 50